<u>HEALTH AND SAFETY EXECUTIVE</u>

<u>RESEARCH AND LABORATORY SERVICES DIVISION</u>

Broad Lane, Sheffield S3 7HQ

Collapse load calculations
for barrier 124A

by   *

Professor R A Smith MA PhD CEng MIM
and
G A C Games BA

IR/L/ME/89/36

*

Department of Mechanical Engineering
University of Sheffield

* Department of Mechanical Engineering
   University of Sheffield

<u>Distribution</u>   Issue authorised by:Dr A Jones

The Court of Inquiry (5 copies)   Date: 7 February 1990
ACC J Mervyn Jones   West Midlands Police
Mr D C T Eves
Mr A Barrel1   TD
Mr P G Jones   TD
Mr M S Nattrass   FAID Area 14
Mr J P Giltrow   HFS (N)
Mr M R Stephenson   NE FCG
Mr M A Fountain   TD 3B
Mr J B Hibbs   NE FCG
Mr M James   TD 3B
Mr C J Pertee   NE FCG
Dr J McQuaid
Dr A Jones
Dr J H Foley   <u>TO RLSD/DIAS STAFF ONLY</u>
Dr C E Nicholson   NOT TO BE COMMUNICATED
Mr P F Heyes   OUTSIDE HSE WITHOUT THE
Mr I R Price   APPROVAL OF THE AUTHORISING
Mr D Waterhouse   OFFICER
Mr G A C Games
Mr G Norton
Authors
RPS   SMR/343/235/01
Library (2)
Registry File   S80.02.OTH.814

CONTENTS

1 INTRODUCTION

During the incident which occurred at Hillsborough Stadium on 15 April 1989, two bays, 2\3 and 3\4, of barrier 124A, Fig 1, were broken down. This report attempts to calculate collapse loads for the barrier and compares these loads with the pressures likely to have been generated by the crowd.

Examination and mechanical testing of the broken barrier by staff of the Health and Safety Executive (HSE), revealed that the upper rail had been manufactured from wrought iron and was probably over sixty years old. The vertical supports were made from mild steel (Ref 1). The tube was attached to the supports by straps, underneath which considerable corrosion of the tube had occurred.

2 MATERIAL PROPERTIES

Tensile tests from 2 specimens taken from the tube gave average tensile strength of 366 MPa, 0.2% proof stress 259 MPa and an estimated elastic limit of 150 MPa. Because of the considerable work hardening which occurs after yield in this material and the sensitivity of the yield stress to prior load history, there is an ambiguity about what single value of yield (or flow) stress should be used to calculate a fully plastic moment.

Two full scale uniform bending tests were carried out on similar wrought iron tubes from barrier 129, as described in Appendix 1. From the experimentally determined plastic collapse loads and the geometry of the tube, representative flow stresses, of, were determined from each test. The values obtained were 298.2 MPa and 290.9 MPa. The difference in the two values of flow stress obtained by experiment gives an indication of the reliability of the material property input to the collapse calculations, i.e. +/- 1.2%. The average of these values, 294.6 MPa was used in the subsequent collapse calculations. This value is some 5.7% less than that obtained by using the approximation of the average of the tensile strength and the 0.2% yield stress obtained in a tensile test. An average value of Young's Modulus, E, (in flexure) of 190.5 GPa was also obtained from these experiments.

3 SECTION PROPERTIES OF THE BARRIER TUBE

Second moments of area, I, for a tube of outside diameter D and uniform wall thickness, t, were calculated from the formula:

$$I = \frac{\pi D^4}{64}\left[1 - \left[1 - \frac{2t}{D}\right]^4\right] \quad \text{- - - - - - - - - - - - - - (1)}$$

Equation (1) and the formulae which follow can be found in standard references (e.g. Ref 2).

Fully plastic moments **Mp** were calculated as a product of the flow stress σ_f and Zp the plastic modulus:

$$Z_p = \frac{D^3}{6}\left[1 - \left[1 - \frac{2t}{D}\right]^3\right] \quad \text{- - - - - - - - - - - - - (2)}$$

The nominal dimensions of the tube, 60 mm outside diameter and 4 mm wall thickness are used in the preliminary calculations in the bent two sections.

4 ELASTIC DEFLECTIONS UNDER TEST LOADING

The elastic deflection(6) at the centre of a beam of length L, built-in at bot ends and subjected to a uniformly distributed load w, is given by

$$\delta = \frac{wL^4}{384EI} \quad \text{- - - - - - - - - - - - - - (3)}$$

If the ends are simply supported, the deflection is increased by a factor of five.

For a span between supports (L) of 2.2 m, the length of spans 2\3 and 3\4 of barrier 124A, subjected to the test loading of 6 kN/m, a figure prescribed by the "Green Guide[n] (Ref 3), a central deflection of 6.9 mm is obtained. If the ends are free, the deflection increases to 34.5 mm. In the calculation which follows, the central span (2\3) of barrier 124A has been treated as having built-in ends. The outer span (3\4), has been treated as having end 3 built-in and end 4 simply supported.

5 YIELDING UNDER TEST CONDITIONS

For the span 2\3, the clamping moments are $wL^2/12$. First yield will occur when these moments equal $2\sigma_y \times I/D$. If σ_y corresponds to the measured elastic limit of the material(150 MPa), then first yield corresponds to 3.4 kN/m or just over half of the test load. 0.2% proof stress gives a first yield load of 5.9 kN/m. Thus some yielding occurs on first loading up to the test load of 6 kN/m. Subsequent loading up to this test load will be elastic because of the strain-hardening capabilities of the material.


6 CALCULATIONS OF PLASTIC COLLAPSE LOADS

The wall thickness of the tube under straps at 2, 3 and 4 was found to be much reduced by corrosion. The reduction in thickness was not uniform round the circumference; calculations of the plastic moduli of the as-measured sections have been made by area integration, described in Appendix 2. The following table results:

	Section dimensions		Plastic modulus	Fully plastic momen (σ_f = 294.6 MPa)
	D mm	t mm	Z_p mm^3	$M_p = \sigma_f \times Zp$ kNm
Tube 2\3 End 2	Corroded		5,007+	1.48
Tube 2\3 Centre	60.80	3.90	12,646*	3.73
Tube 2\3 End 3	Corroded		8,279+	2.44
Tube 3\4 End 3	Corroded		8,504+	2.51
Tube 3\4 Centre	60.40	3.90	12,398*	3.65
Tube 3\4 End 4	Corroded		8,269+	2.44

+ By area integration from measured irregular cross section(Appendix 2)
* By Equation (2)

The general case of plastic collapse for a beam of length L is shown below:

$$w \text{ / unit length}$$
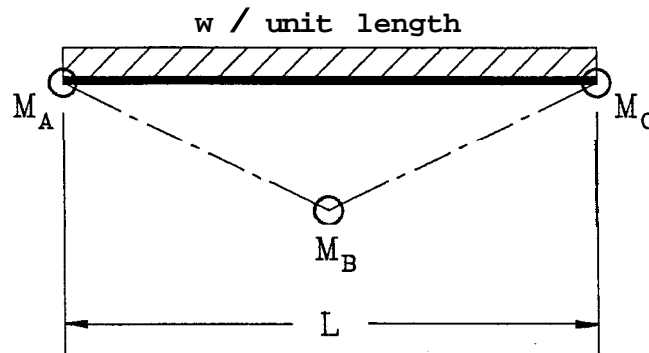
where M_A and M_C are the moments at the supports and M_B is the moment at the centre of the beam. The collapse load is

$$w_c = \frac{4 \times (M_A + 2M_B + M_C)}{L^2} \qquad - - - - - - - - - - - - - - - (4)$$

The standard case we take is for the original beam built-in at both ends, i.e. span 2\3 of barrier 124A. Denoting the collapse load for this case as w_c and noting $M_A = M_C = M_B = M_p$, the fully plastic moment at the uncorroded centre,

$$w_c = \frac{16 \times M_p}{L^2} = \frac{16 \times 3.73}{2.2^2} = 12.3 \text{ kN/m}$$

Now for the span 3\4, assuming end 4 to be simply supported, the calculation above can be repeated with $M_C = 0$, and $M_A = M_B = 3.65$ kNm, giving a collapse load of 9.05 kN/m.

For the spans in a corroded condition, the central plastic moment can be assumed to remain unchanged, but the appropriate plastic moments in the above table can be substituted for end moments. The following table results:

	Collapse Loads: kN/m	
	Built-in (Span 2\3)	One end simply supported (Span 3\41 ($M_C = 0$)
Original thickness	12.3 (2.1)	9.05 (1.51)
Corroded condition	9.40 (1.57)	8.11 (1.35)

The figures in brackets are the calculated collapse loads as multiples of the test load (6 kN/m).

For the unsymmetrical calculations in the previous table, the inner plastic hinge does not occur exactly at the centre of the span. The effect of this on the calculated collapse loads is negligible and smaller than other sources of uncertainty.

Tests performed by Dr Eastwood (Ref 4) on a similar, but not identical barrier, after the incident, showed that a load of 9 kN/m (test load x 1.5) was sufficient to cause very large permanent deformation of the tube. The calculated collapse loads therefore appear to be realistic values.

7   COLLAPSE MODE

If we assume the shear strength to be only 50% of the tensile strength, then to shear a 1.5mm wall thickness of tube directly, a load of 48 kN/m is required. Even the worst corroded end had an average wall thickness of this value, yet the shear failure load is many times higher than the plastic collapse load. This evidence, together with the bent shape of the tube after the incident, supports the view that barrier failure occurred by plastic collapse of the tube. Because of its position, span 3\4 would fail before span 2\3. If collapse of the legs had taken place prior to the failure of the tube, the tube would not have been bent in the manner which was observed. Thus, of the loads calculated in Section 6, the value of collapse for span 3\4 in the corroded condition governs the problem.

8   ESTIMATES OF CROWD FORCES ACTING ON BARRIERS

A theoretical model of the forces generated by a crowd behind a barrier has been developed, see Appendix 3. Values from this model are shown on Fig 2, onto which values for the various calculated collapse loads have been added. For a crowd density of 8/sq m, measured from photograhs (Ref 1), span 3\4 in the original condition would withstand a crowd depth of approximately 6.4 m before collapse. This would reduce to 6 m if it were in the corroded condition. Because span 3\4 of barrier 124A was unprotected by barrier 136, a crowd of 7 m was able to exert pressure on this part of the barrier. Given that the crowd was not of uniform density throughout and the approximate nature of the crowd loading model, these figures adequately explain the collapse of the barrier. Once span 3\4 had failed, span 2\3 would become simply supported at end 3 and the vertical support would twist, causing collapse of span 2\3 at a similar load level. If the crowd had been restricted to 5.4/sq m, the crowd depth to cause collapse would be 8 m and 7.5 m in the original and corroded conditions respectively. This latter value is in excess of the depth of crowd at this location and indicates that the span would have survived had the crowd density been so restricted.

If barrier 136 had been complete, the crowd depth behind barrier 124A would have been limited to 3.5 m depth. The maximum load generated, as predicted by the 'leaning crowd' model, by a crowd as dense as 10/sq m would have been some 20% less than the test load.

Given that the gap in the row of barriers behind 124A was greater than that recommended in the Green Guide (Ref 5), the test load of *6 kN*/m was inadequate. At 5.4/sq m the model predicts that a crowd of 7 m depth would generate a load some 22% greater than the test load.

9   CONCLUSIONS

9.1   Collapse loads have been calculated for the spans 2\3 and 3\4 of barrier
      124A which was broken down during the Hillsborough Stadium incident.

9.2   If the barriers had been of the original thickness at the supports, loads
      of 2.1 and 1.51 times the test load of *6* kN/m would have been needed to
      collapse the barrier at spans 2\3 and 3\4 respectively. With the reduced
      wall thicknesses as measured, these ratios fall to 1.57 and 1.35 x test
      load.

9.3   These figures have been compared with barrier loads generated from a
      'leaning crowd model.

9.4   In the corroded condition for a crowd of measured density 8/sq m, the
      span 3\4 of the barrier would have been broken down by a crowd of
      approximately *6* m depth behind the barrier. A crowd of some 7 m depth
      existed directly behind span 3\4.

9.5   If a crowd density of 5.4/sq m is assumed, the same tube would have
      required about 7.5 m of crowd to break it down.

10   REFERENCES

(1) The Hillsborough Incident 15 April 1989: An Investigation into Various
Technical Aspects prepared for the Court of Inquiry. C E Nicholson, HSE Report
No IR/L/ME/MM/89/1,   June 1989.

(2) Steel Designers Manual: The Steel Construction Institute; Crosby Lockwood
and Son Ltd

(3) Guide to Safety at Sports Grounds: Home Office/Scottish Office; HMSO, 1986.

(4) Statement by Dr W Eastwood submitted to the Court of Inquiry, page 48

(5) An Estimation of the Maximum Allowable Capacity of Pens 3 and 4.
A L Collins, D Waterhouse, HSE Report No IR/L/ME/89/35
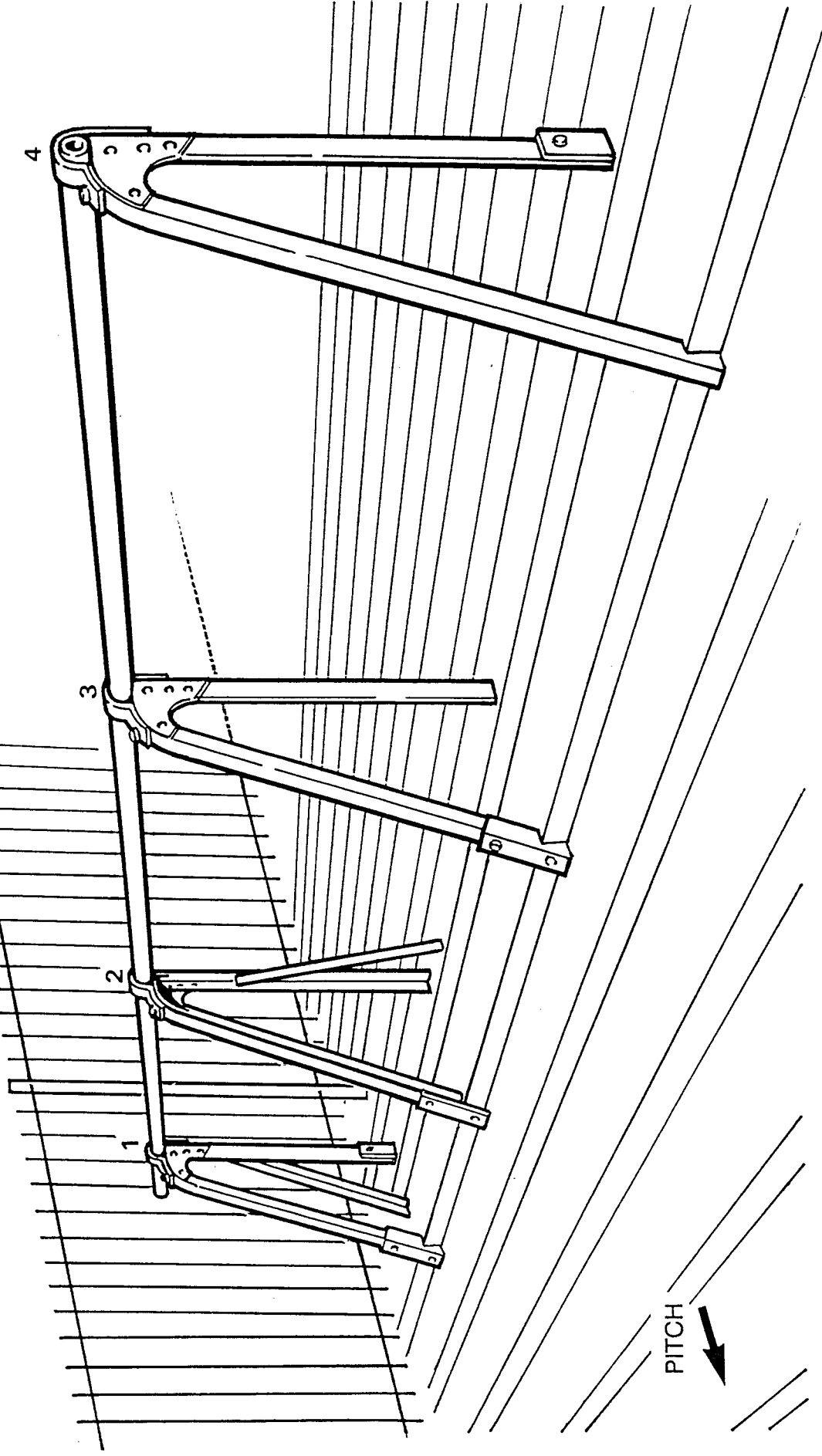
RADIAL FENCE BETWEEN
PENS 2 & 3

4

3

2

1

PITCH

Fig. 1 - Reconstruction of Barrier 124A
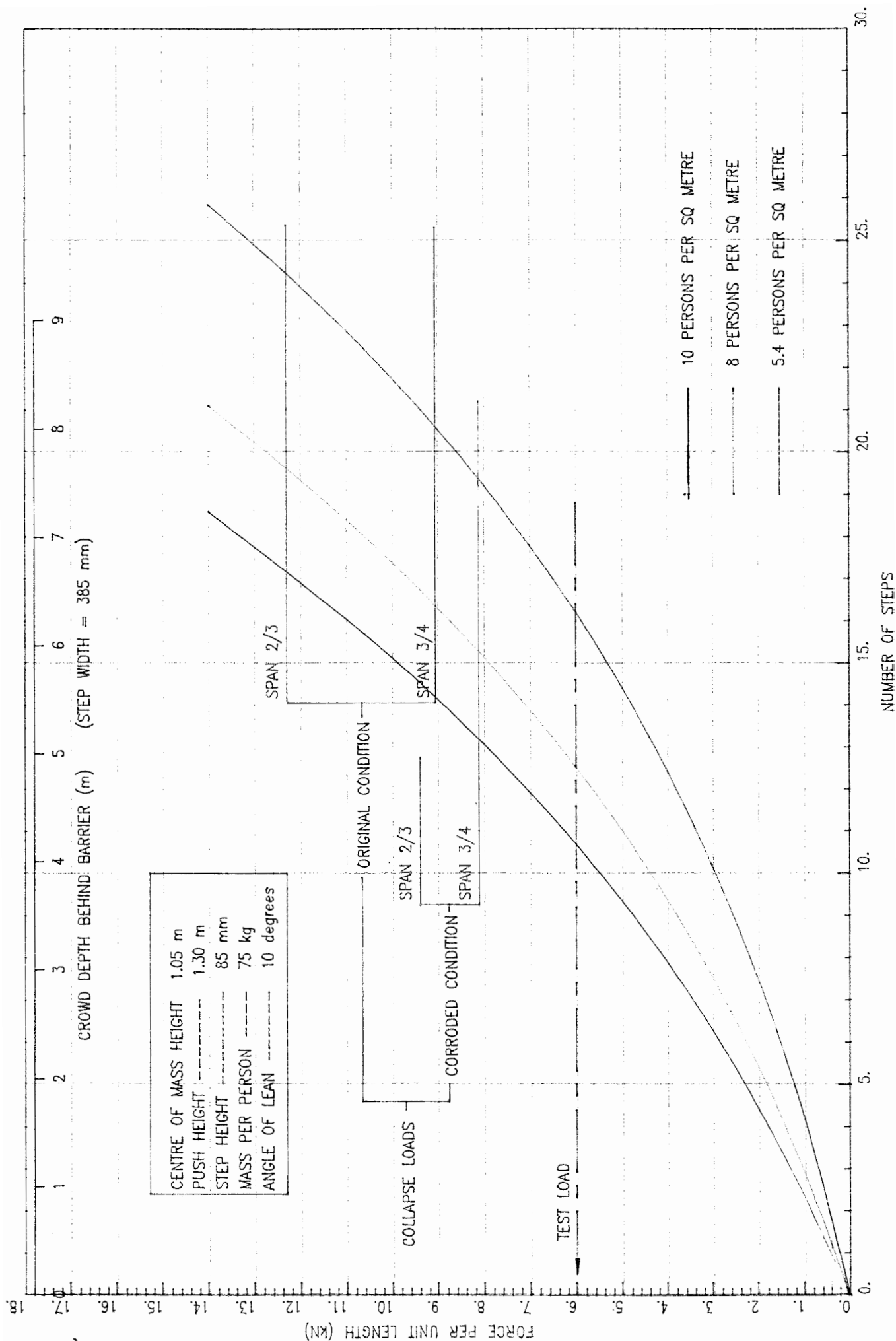
FIG. 2   COMPARISON OF CALCULATED COLLAPSE LOADS AND CROWD FORCES

APPENDIX 1

<u>BENDING TESTS TO DETERMINE THE MECHANICAL PROPERTIES OF THE WROUGHT
IRON TUBULAR TOP RAIL FROM BARRIER 129</u>

<div align="center">
by

A L Collins
K Heenan
J C Moore
D Waterhouse
</div>

A1.1 <u>THE NEED FOR BENDING TESTS</u>

Calculations of the loading to cause the collapse of barrier 124A requires a
knowledge of the mechanical properties of the wrought iron used in spans 2\3
and 3\4 of the top rail of the barrier.

RLSD's Metallurgy and Materials Section conducted tensile tests on two
specimens cut from the wrought iron tube used in spans 2\3 and 3\4 of barrier
124A. However, there were reservations about the use of the results of these
tests in calculations of the collapse load of this barrier because:

(i> tests conducted on small specimens of a material that is known to have a
     heterogeneous structure may not provide results that are representative
     of a large sample;

(ii) the tubes that had formed spans 2/3 and 3/4 were found to be permanently
      bent when they were recovered after the incident; it is known that the
      yield stress of wrought iron is likely to be affected by its previous
      loading history, and that wrought iron is sensitive to post-yield
      strain-hardening;

(iii) bending moments introduce compressive stresses as well as tensile
      stresses into the tube; we did not have data about the compressive
      properties of wrought iron that could be applied with reasonable
      confidence in calculations of the collapse load of barrier 124A.

It was the opinion of Smith and Games that data obtained from a bending test on
an undeformed sample of a similar wrought iron tube would be likely to be more
representative than the data obtained from tensile tests on small specimens.

A1.2 <u>SELECTION OF THE TEST SAMPLE</u>

Barrier 129 was a six-span barrier situated in the North-West Pen (Pen 5) of the
West terraces. It appeared to be of a similar construction to barrier 124A and
its top rail was not obviously bent. We assisted in the removal of the
complete assembly of barrier 129 from the West terraces to RLSD's premises.
Mr J G Tattersall of RLSD's Metallurgy and Materials Section confirmed that
the length of the top rail selected for testing was made from wrought iron.

A1.3   METHOD OF TESTING AND CALCULATION OF THE REQUIRED DATA
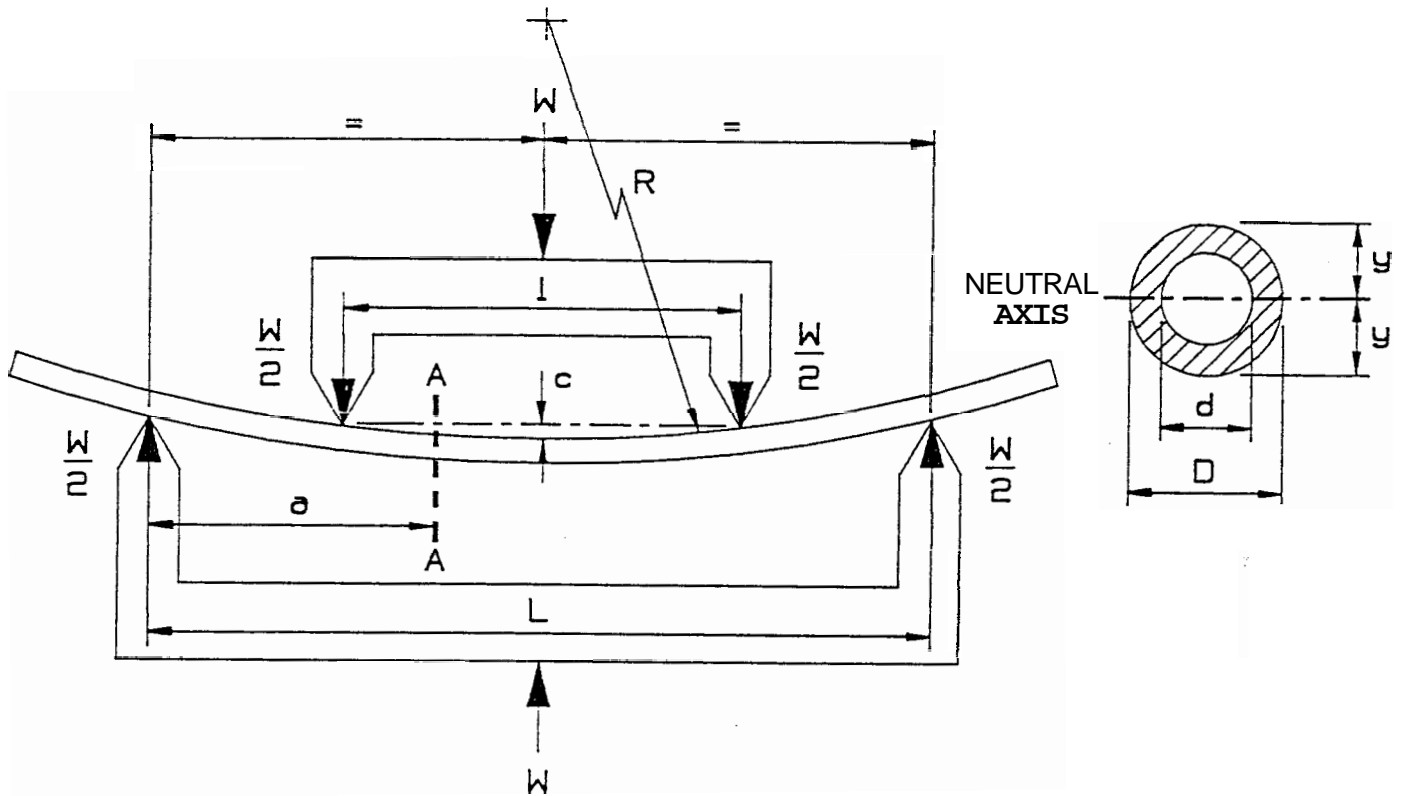
Fig A1.1   Symmetrical 4-point loading of a beam

Bending Moment (M) at a section A-A of the beam:

$$M = \frac{W \times a}{2} \quad \text{for } a \leqslant (L/2 - 1/2); \qquad \text{i.e. greatest value of } M = \frac{W \times (L - 1)}{4}$$

$$\text{and } M = \frac{W \times a}{2} - \frac{W}{2}\left[a - \frac{(L - 1)}{2}\right] \quad \text{for } (L/2 - 1/2) \leqslant a \leqslant (L/2 + 1/2)$$

$$= \frac{W \times (L - 1)}{4}$$

$$\text{and } M = \frac{W \times (L - a)}{2} \quad \text{for } a \geqslant (L/2 + 1/2); \quad \text{i.e. greatest value of } M = \frac{W \times (L - 1)}{4}$$

The greatest bending moment is therefore imposed along the full length of the central span (1) of the beam and has a uniform value of:

$$M = \frac{W \times (L - 1)}{4} \qquad \text{- (1)}$$

Determination of the yield stress of the material

The elastic bending equation is expressed as:

$$\frac{M}{I} = \frac{\sigma}{y} = \frac{E}{R} \qquad - \quad (2)$$

where M is the bending moment applied to the beam
    I is the second moment of area of the cross-section
    a is the fibre stress on the material of the beam
    y is the distance of a fibre from the neutral axis
    E is Young's Modulus for the material of the beam
    R is the radius of curvature of the neutral axis at the cross-section
    considered

The second moment of area (I) for a circular section tube can be shown to be:

$$I = \frac{\pi \times (D^4 - d^4)}{64} \qquad - - - - - - - - - - - - - - - - - - \quad (3)$$

where D and d are the outer and inner diameters, respectively, of the tube

$$\text{from (2)} \quad \sigma = \frac{M \times y}{I} \qquad - - - - - - - - - - - - - - - - - - \quad (4)$$

Equation (4) shows that as the bending moment is increased the outermost fibres will be the first to reach the yield stress (σ_y) of the material. The relationship between load and deflection will cease to be linear when the outermost fibres are subjected to the yield stress of the material. Plastic deformation will be initiated and will spread inwards towards the neutral axis if the bending moment continues to increase. The outermost fibres of a hollow circular section of outer diameter D are situated at a distance D/2 from the neutral axis, i.e. y = D/2.

$$\sigma_y = \frac{M_y}{I} \times \frac{D}{2} \qquad - \quad (5)$$

where M_y is the bending moment at which yielding commences

Substituting for M_y from (1) and I from (3) in (5)

$$\sigma_y = \frac{8 \times W_y \times (L - 1) \times D}{\pi \times (D^4 - d^4)} \qquad - - - - - - - - - - - - - - - - - - - \quad (6)$$

where σ_y the yield stess
    W_y is the load when yielding commences, i.e. the load at which the graph
    relating force and deflection ceases to be linear

Therefore, if W_y can be obtained from the force\deflection graph, the yield stress (σ_y) can be determined.

Determination of Young's Modulus (E) for the material

$$\text{From (2)} \qquad E = \frac{M \times R}{I} \qquad \cdots \cdots \cdots \cdots \cdots \cdots \cdots \cdots \quad (7)$$

E and I are both constants, therefore R is proportional to M. Equation (1) shows that M is uniform over the central span (1) of the beam. Provided the loaded beam remains in an elastic condition, its radius of curvature R over the central span will also be uniform i.e. the deflected shape of the central span will be an arc of a circle.

From the geometrical properties of a circle it can be shown that if $1 \gg c$:

$$R = \frac{1^2}{8 \times c} \qquad \text{- (8)}$$

where R is the radius of curvature of the central span
       1 is the length of the central span
       c is the mid-span deflection of the central span

substituting for M from (1), I from **(3),** and R from (8) in (7)

$$E = W/c \times \frac{2 \times (L - 1) \times 1^2}{\pi \times (D^4 - d^4)} \qquad \text{- (9)}$$

W/c is the gradient of the elastic, linear region of the load-deflection curve, which can be measured from the graph obtained from the bending test. The remaining terms in Equation (9) are known constants and therefore E can be evaluated.

Comparison of theoretical and experimental maximum bending strengths

Appendix 2 expresses the maximum theoretical bending strength (M_p) of a beam in the form:

$$M_p = \sigma_l \times Z_p \qquad \text{- (10)}$$

σ_l is a limiting constant stress which, dependent upon the properties of the material of the beam, may be the yield stress (σ_y) or a 'flow stress' (σ_f).

Z_p is a plastic section modulus, which for a hollow circular section of uniform wall thickness (t) may be expressed in terms of its outer and inner diameters, or in terms of its outer diameter and wall thickness.

$$Z_p = \frac{(D^3 - d^3)}{6} = \frac{D^3}{6}\left[1 - \left(1 - \frac{2t}{D}\right)^3\right] \quad \text{- - - - - - - - - - - - - - - - - - (11)}$$

Therefore

$$M_p = \sigma_l \times \frac{D^3}{6}\left[1 - \left(1 - \frac{2t}{D}\right)^3\right] \quad \text{- - - - - - - - - - - - - - - - (12)}$$

If an appropriate value is known for σ_l, then the theoretical maximum bending strength may be calculated from Equation (12) and its value compared with the experimental maximum bending strength obtained from the test to check the validity of the calculation.

Equipmentfor conducting the bending tests

We designed and constructed equipment of the type shown diagrammatically in Fig Al.l that was suitable for installation in RLSD's 1 MN (100 tonf) tension\compression testing machine. The equipment was designed to accept a sample with an overall span of 2 m and a central span of lm, the objective being to minimize the point loads applied to the tube within the constraints imposed by:

(i)   the overall length of sample available for testing;
(ii)   the loading range of the testing machine;
(iii)   maximizing the length of tube subjected to a uniform bending moment
        in order to obtain representative results

A spring-tensioned potentiometric displacement transducer was used to measure deflections of the tube. The transducer had a range of 760 mm and was actuated by a flexible wire, the end of which was attached to the mid-span of the tube. The transducer was mounted on the loading rig so as to measure deflections of the central span between its loading points.

The output from the potentiometric transducer was connected to a digital voltmeter and the assembly calibrated and adjusted to provide a direct digital reading of displacement, in millimetres, with a resolution of 0.1 mm. The calibrated testing machine was operated on the lowest range of 100 kN, the force being displayed in digital form with a resolution of 0.1 kN. Fig Al.2 shows a general view of the assembled equipment prior to conducting a test.

The testing machine was controlled manually whilst simultaneous readings were taken of force and deflection. Fig Al.3 shows a sample in an advanced stage of plastic deformation. Two samples from the top rail of barrier 129 were tested, and the force\deflection graphs obtained from the results of these tests are shown in Figs Al.4 and Al.5.

Values of yield stress, Young's Modulus, and maximum bending moment were calculated for both samples of tube, using data on the force\deflection graphs and Equations (6), (9) and (1) respectively. The theoretical maximum bending

moment for each sample was also calculated using Equation (12) with $\sigma_l = \sigma_y$, the yield stress determined from the same bending test.

A1.4 RESULTS OBTAINED FROM THE BENDING TESTS MADE ON SAMPLES FROM BARRIER 129

	Sample No 1 Fig A1.4	Sample No 2 Fig A1.5
Outer diameter	60.13 mm	60.43 mm
Inner diameter	51.61 mm	52.08 mm
Wall thickness	4.26 mm	4.18 mm
Yield stress (Equation 6)	256.1 MPa (16.6 tonf/sq in)	244.6 MPa (15.8 tonf/sq in)
Young's Modulus (Equation 9)	193.6 GPa (12,500 tonf/sq in)	187.4 GPa (12,100 tonf/sq in)
Theoretical max bending moment (Equation 12)	3,413 Nm (1.12 tonf ft)	3,237 Nm (1.07 tonf ft)
Experimental max bending moment (Equation 1)	3,975 Nm (1.31 tonf ft)	3,850 Nm (1.27 tonf ft)

The theoretical maximum bending moments were 15% and 16% less than the experimental maximum bending moments obtained from Samples 1 and 2 respectively. It was the opinion of Smith and Games that these discrepancies were too great to justify using the experimentally determined yield stresses to calculate the collapse load of barrier 124A.

They decided to use a 'flow stress' in their calculations of the collapse load of barrier 124A. The 'flow stresses' of Samples 1 and 2 were obtained by transposing Equation (10) into the form:

$$\sigma_f = \frac{M_e}{Z_p} \quad - \quad (13)$$

where σ_f is the 'flow stress' for the material
M_e is the maximum bending moment determined experimentally from a bending test

The 'flow stresses' obtained from the bending tests made on samples taken from barrier 129 are shown in the following Table:

Sample No	'Flow stress' (σ_f)
1	298.2 MPa (19.3 tonf/sq in)
2	290.9 MPa (18.8 tonf/sq in)
Mean value	294.6 MPa (19.1 tonf/sq in)
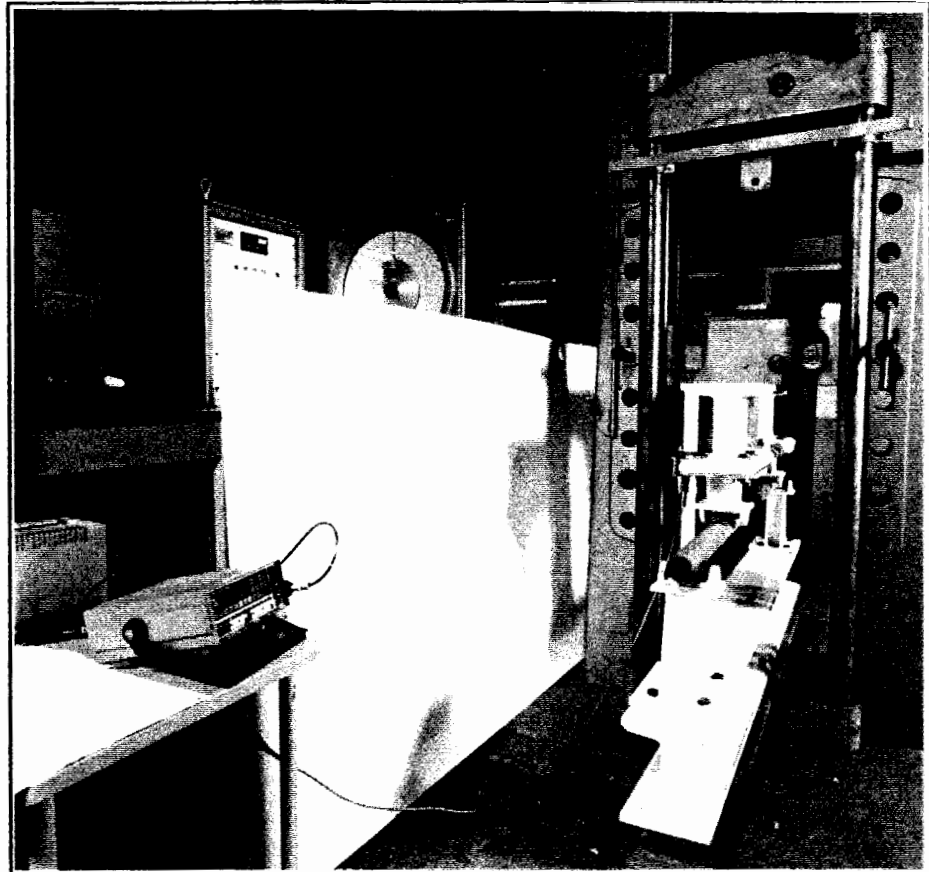
9001-008/2

Fig.AI.2 - View of the bending equipment and the sample prior to testing
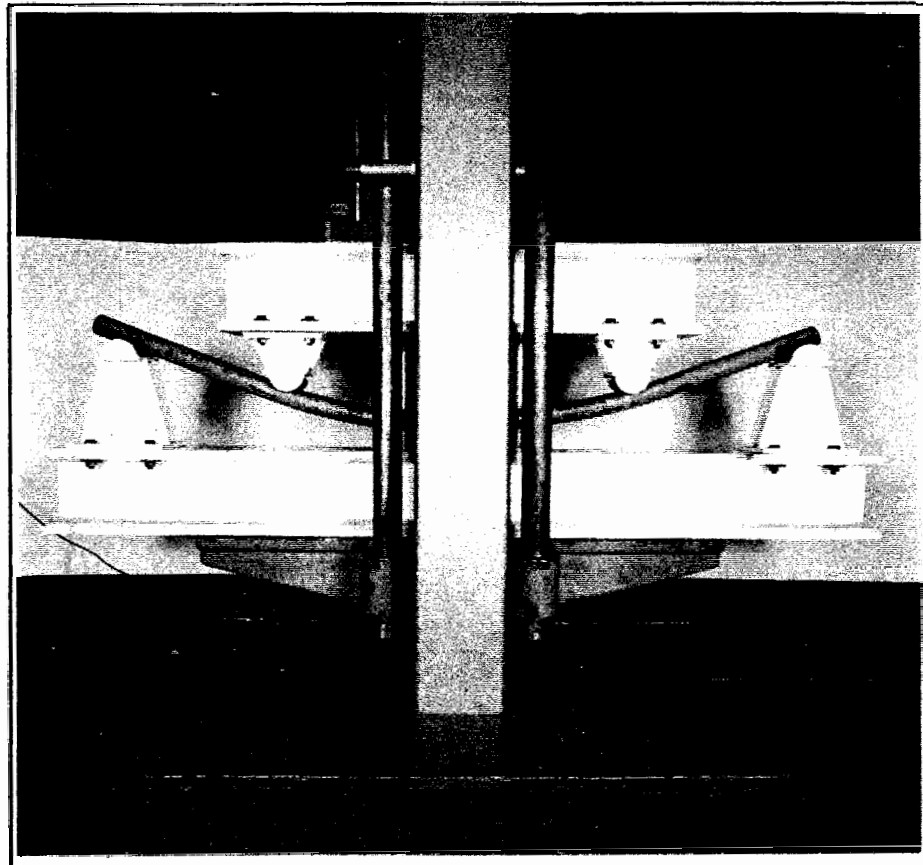
9001-008/4

Fig.AI.3 - View of the bending equipment with the sample at an advanced stage of plastic deformation

Graph Ref [300,3]HILYIELD3.PLT

OUTSIDE DIAMETER MEASURED AT MID-SPAN   60.128 mm

INSIDE DIAMETER MEASURED AT MID-SPAN   51.605 mm

TUBE UNDER TEST IN
4 POINT BENDING

APPLIED LOAD

1m

2m

APPLIED LOAD

BEGINNING OF YIELD 10.0 kN

GRADIENT OF GRAPH IN ELASTIC REGION = 1.818 kN/mm.

DEFLECTION AT BEGINNING OF YIELD 5.5 mm

LOAD (kN)

DISPLACEMENT (mm)
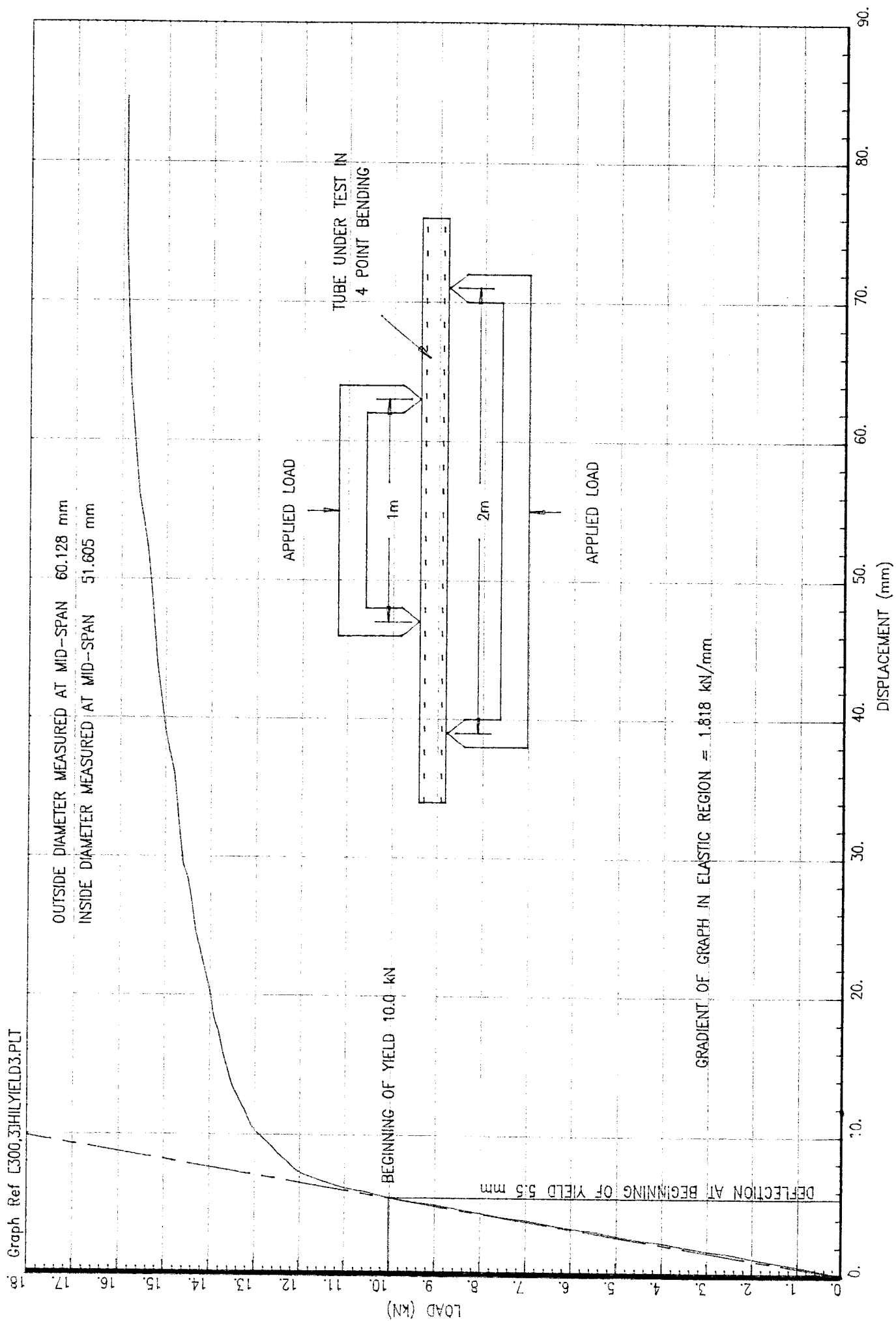
Fig A1.4   LOAD DEFLECTION CURVE OF 1st WROUGHT IRON TUBE FROM BARRIER No.129

Graph Ref [300.3]HILYIELD4.PLT

OUTSIDE DIAMETER MEASURED AT MID-SPAN 60.425 mm

INSIDE DIAMETER MEASURED AT MID-SPAN 52.075 mm

TUBE UNDER TEST IN
4 POINT BENDING

APPLIED LOAD

APPLIED LOAD

1m

2m

BEGINNING OF YIELD 9.5 kN

DEFLECTION AT BEGINNING OF YIELD 5.4 mm

GRADIENT OF GRAPH IN ELASTIC REGION = 1.759 kN/mm

LOAD (kN)

DISPLACEMENT (mm)

Fig A1.5   LOAD DEFLECTION CURVE OF 2nd WROUGHT IRON TUBE FROM BARRIER No.129

<u>APPENDIX 2</u>

<u>EVALUATION OF THE PLASTIC SECTION MODULUS OF CROSS-SECTIONS FROM
SPANS 2\3 AND 3\4 OF BARRIER 124A</u>

by

A L Collins
and
D Waterhouse

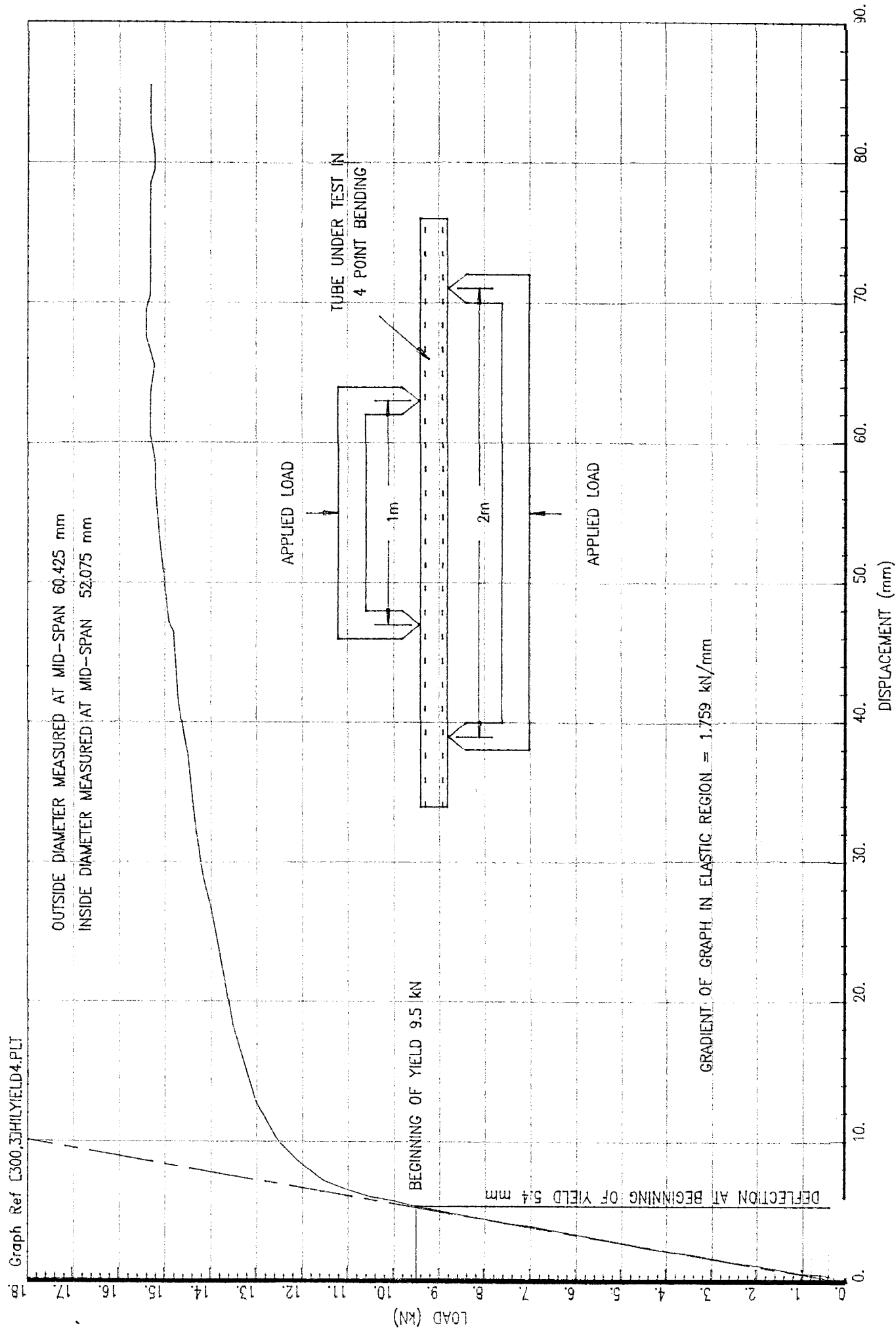A2.1 <u>PREDICTION OF THE PLASTIC COLLAPSE OF A BEAM</u>

Bending moments are produced on a beam by the load that it is supporting.
These bending moments are resisted by moments of resistance produced by
tensile and compressive stresses developed on the cross-sectional area of the
beam.

A beam of ductile material, with a span that is large in comparison to its
cross-sectional dimensions, will fail by plastic collapse when the bending
moment creates sufficient plastic hinges along its span to transform the beam
from a structure to a mechanism. A plastic hinge is formed when the tensile
and compressive stresses exceed the yield strength of the material throughout
the depth of the beam's cross-section.

If the moments of resistance that are developed at the plastic hinges can be
determined, then the principle of Virtual Work may be used to calculate the
bending moment, and therefore the loading, that will cause the beam to
collapse.

Simple plastic theory expresses the maximum moment of resistance (M_p) that can
be developed by a cross-section of a beam(its maximum plastic moment of
resistance) as the product of its plastic section modulus (Z_p) and a limiting
constant value of stress (σ_l).

i.e. $M_p = \sigma_l \times Z_p$ - (1)

This relationship makes the following assumptions about the material of the
beam:

(i)   an idealized rigid-plastic relationship exists between stress and strain,
i.e. deformation does not occur until a limiting value of stress (σ_l) is
reached, after which large deformations are developed whilst this stress
remains constant;

(ii) the behaviour of the material is the same in compression as in tension.

The tensile yield stress of the material (σ_y) is commonly used in Equation (1)
when strain-hardening(work-hardening) of the material may be neglected. When
strain-hardening of the material cannot be ignored then it is customary to use
a 'flow stress' (σ_f) having a value between the yield stress and the ultimate
stress.

i.e. $\sigma_l = \sigma_y$ (strain-hardening neglected)
or $\sigma_l = \sigma_f$ (strain-hardening included)

Experience has shown that this simple plastic theory can predict the failure of beams by plastic collapse with an accuracy that is acceptable for practical purposes.

A2.2 DETERMINATION OF THE PLASTIC SECTION MODULUS

If the material of a section that is subjected to pure bending exhibits the same ideal rigid-plastic behaviour in both tension and compression, then Z_p can be shown to be equal to the First Moment of Area of the cross-section about its neutral axis (or unstrained fibre). Furthermore, in these circumstances, the neutral axis will coincide with the centroid of the area of the cross-section.

The fully plastic section modulus for a hollow circular cross section of ideal rigid-plastic material and uniform wall thickness can be shown to be either:

$$Z_p = \frac{D^3 - d^3}{6}$$

where D = outer diameter
and d = inner diameter

$$\text{or } Z_p = \frac{D^3}{6}\left[1 - \left(1 - \frac{2t}{D}\right)^3\right] \quad\text{- (2)}$$

where t = wall thickness

Mr J G Tattersall of RLSD's Metallurgy and Materials Section had made ultrasonic measurements of the wall thicknesses of the wrought iron tube that had formed the top rail of crush barrier 124A. These measurements caused us to conclude that it was reasonable to use Equation (2) to calculate Z_p for the top rail in the mid-span region of spans 2\3 and 3\4 of barrier 124A. The measured dimensions and their corresponding plastic section moduli are shown in the following Table.

Mid-span	Outer diameter (D)	Inner diameter (d)	Wall thickness (t)	Plastic section modulus (Z_p)
	mm	mm	mm	mm^3
2\3	60.80	53.00	3.90	12,646
3\4	60.40	52.60	3.90	12,398

Both ends of the tubular sections that had formed spans 2\3 and 3\4 had fractured; the ends of the spans were deformed, severely corroded, and had variable wall thicknesses. It was our opinion that the variability of the wall thicknesses rendered Equation (2) unsuitable for calculating values of Z_p at the ends of spans 2\3 and 3\4, and that these values would have to be determined by numerical integration.

Mr Tattersall provided us with sketches that showed wall thicknesses at the fractured ends of spans 2\3 and 3\4. We used a computer-aided draughting(CAD) system to draw our best impression of the cross-section at each end of spans 2\3 and 3\4 before deformation failure occurred. Our re-construction of the cross-sections are shown in Figs A2.1 to A2.4.

We used the facilities of the CAD system to assist us with the numerical integrations. Each cross-section was divided into strips of 2 mm width, with the exception of the last strip whose width was determined by the outer dimension of the section. A vertical axis was then drawn in the estimated position of the centroid(neutral axis). Each elemental area of tube thickness, with the exception of those adjacent to the estimated position of the centroid was successively magnified by the CAD system and then accurately cross-hatched. The CAD system then automatically calculated the area of each cross-hatched element.

The sum of the elemental areas to the right of the estimated centroidal axis were compared with the sum of those to the left; the centroidal axis being in its correct position when it divides the cross-sectional area into two equal parts. The position of the centroidal axis was adjusted and the process repeated iteratively until the areas to the right and the left of the axis were equal.

Each known elemental area of the tubular wall was then mutiplied by its distance from the centroidal axis to obtain the First Moment of Area of each element. A summation of the First Moments of Area for all the elements provided total First Moment of Area for the complete cross-section. The results obtained during successive stages of the calculation are tabulated in Figs A2.1 to A2.4.

The plastic section moduli that we obtained by numerical integration of the re-constructed cross-sections at the ends of spans 2\3 and 3\4 from barrier 124A are shown in the following Table.

Span	End	Z_p mm^3
2\3	2	5,007
2\3	3	8,279
3\4	3	8,504
3\4	4	8,269

TOP

PITCH SIDE

SPECTATOR SIDE

0.61   1.35

0.65   2

A
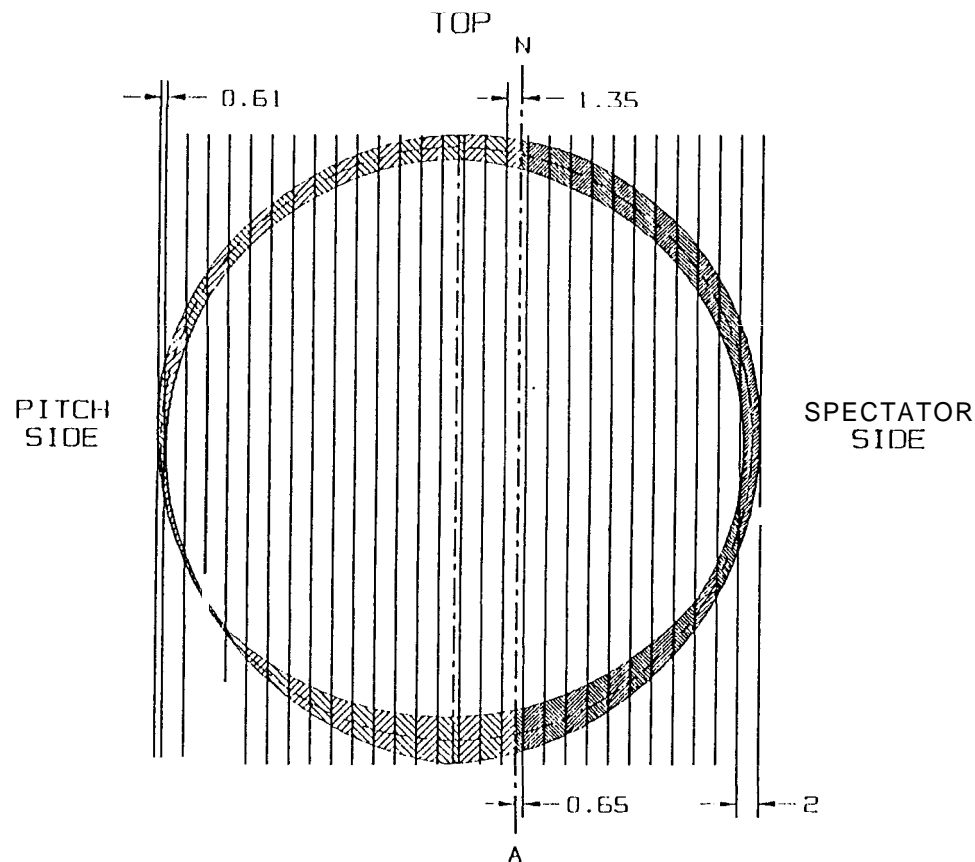
TOTAL PLASTIC SECTION MODULUS = 5006.78 mm^3

RIGHT HAND SIDE

No	AREA (Al)	L (mm)	AREA (Ab)	(Al+Ab)xL	TOTAL
1	1.779	0.325	2.659	1.442	–
2	5.735	1.65	8.046	22.739	24.181
3	6.183	3.65	7.894	51.381	75.562
4	6.531	5.65	7.618	79.942	155.504
5	6.711	7.65	7.372	107.964	263.468
6	6.900	9.65	7.109	135.187	398.655
7	7.203	11.65	6.801	163.147	561.802
8	7.645	13.65	6.362	191.196	752.997
9	8.278	15.65	5.917	222.152	975.149
10	9.149	17.65	5.825	264.291	1239.440
11	11.815	19.65	8.080	390.937	1630.377
12	27.28	21.65	–	590.612	2220.989

TOTAL 2220.989

LEFT HAND SIDE

No	AREA (Al)	L (mm)	AREA (Ab)	(Al+Ab)xL	TOTAL
1	3.568	0.675	5.529	6.140	–
2	5.055	2.35	8.469	31.781	37.921
3	4.812	4.35	8.667	58.634	96.555
4	4.602	6.35	8.646	84.125	180.680
5	4.456	8.35	8.247	106.070	286.750
6	4.338	10.35	7.665	124.231	410.981
7	4.322	12.35	7.095	141.000	551.981
8	4.298	14.35	6.471	154.535	706.516
9	4.231	16.35	6.013	167.489	874.006
10	4.271	18.35	5.348	176.509	1050.515
11	4.242	20.35	4.586	179.650	1230.164
12	4.313	22.35	3.795	181.214	1411.378
13	4.459	24.35	2.850	177.974	1589.352
14	4.704	26.35	1.705	168.877	1758.229
15	5.140	28.35	1.256	181.327	1939.556
16	6.038	30.35	1.489	228.444	2168.000
17	9.345	32.35	4.386	444.198	2612.198
18	5.158	33.655	–	173.592	2785.791

TOTAL 2785.791

Fig A2.1   BARRIER No 124A SPAN 2/3 ,END No 2

TOP

N

0.28 —|←

0.55 —|←

SPECTATOR
SIDE

PITCH
SIDE

—|←— 1.45

—|←— 2

A
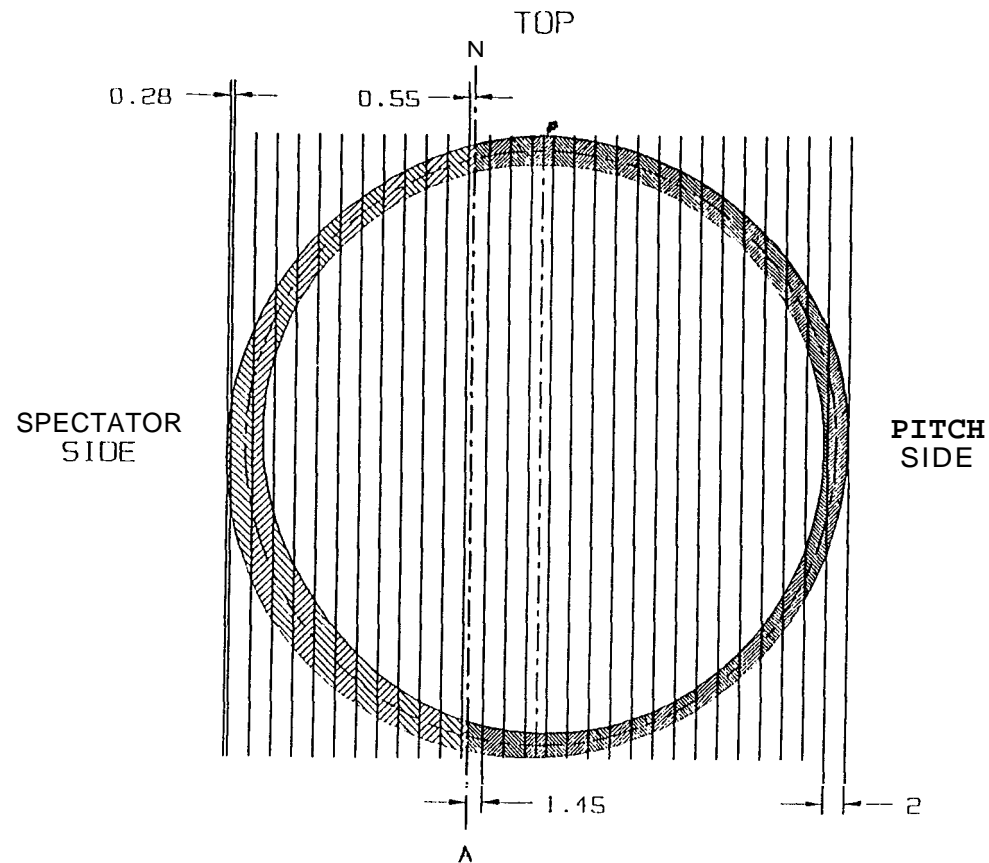
TOTAL PLASTIC SECTION MODULUS = 8278.557 mm^3

RIGHT HAND SIDE

No	AREA (AL)	L (mm)	AREA (Ab)	(AL+Ab)xL	TOTAL
1	3.768	0.725	3.942	5.590	–
2	5.234	2.45	5.110	25.343	30.933
3	5.162	4.45	4.856	45.915	76.848
4	5.572	6.45	4.623	65.758	142.605
5	5.540	8.45	4.434	84.280	226.886
6	5.474	10.45	4.279	101.919	328.805
7	5.488	12.45	4.169	120.230	449.034
8	5.531	14.45	4.087	138.980	588.014
9	5.618	16.45	4.106	159.960	747.974
10	5.704	18.45	4.130	181.437	929.411
11	5.920	20.45	4.265	208.283	1137.695
12	8.226	22.45	4.416	283.813	1421.508
13	8.553	24.45	4.786	326.139	1747.646
14	7.174	26.45	5.323	330.546	2078.192
15	8.189	28.45	6.209	409.623	2487.815
16	10.069	30.45	7.948	548.618	3036.432
17	15.665	32.45	14.008	962.889	3999.321
18	28.033	34.45	–	965.737	4965.058
				TOTAL	4965.058

LEFT HAND SIDE

No	AREA (Al)	L (mm)	AREA (Ab)	(AL+Ab)xL	TOTAL
1	1.431	0.275	1.553	0.821	–
2	5.203	1.55	5.900	17.210	18.031
3	5.271	3.55	6.396	41.418	59.449
4	5.337	5.55	7.011	68.531	127.980
5	5.190	7.55	7.797	100.317	228.297
6	5.027	9.55	8.661	138.360	366.658
7	6.208	11.55	9.857	185.551	552.208
8	7.018	13.55	11.728	254.008	806.217
9	8.267	15.55	14	350.761	1156.978
10	10.795	17.55	17.258	492.330	1649.308
11	18.885	11.55	25.606	871.363	2520.671
12	13.597	21.55	20.921	743.863	3264.534
13	2.158	22.69	–	48.965	3313.499
				TOTAL	3313.499

Fig A2.2   BARRIER No 124A SPAN 2/3 END No 3

TOP

N

1.776

0.3

SPECTATOR SIDE

PITCH SIDE

1.7

2

A
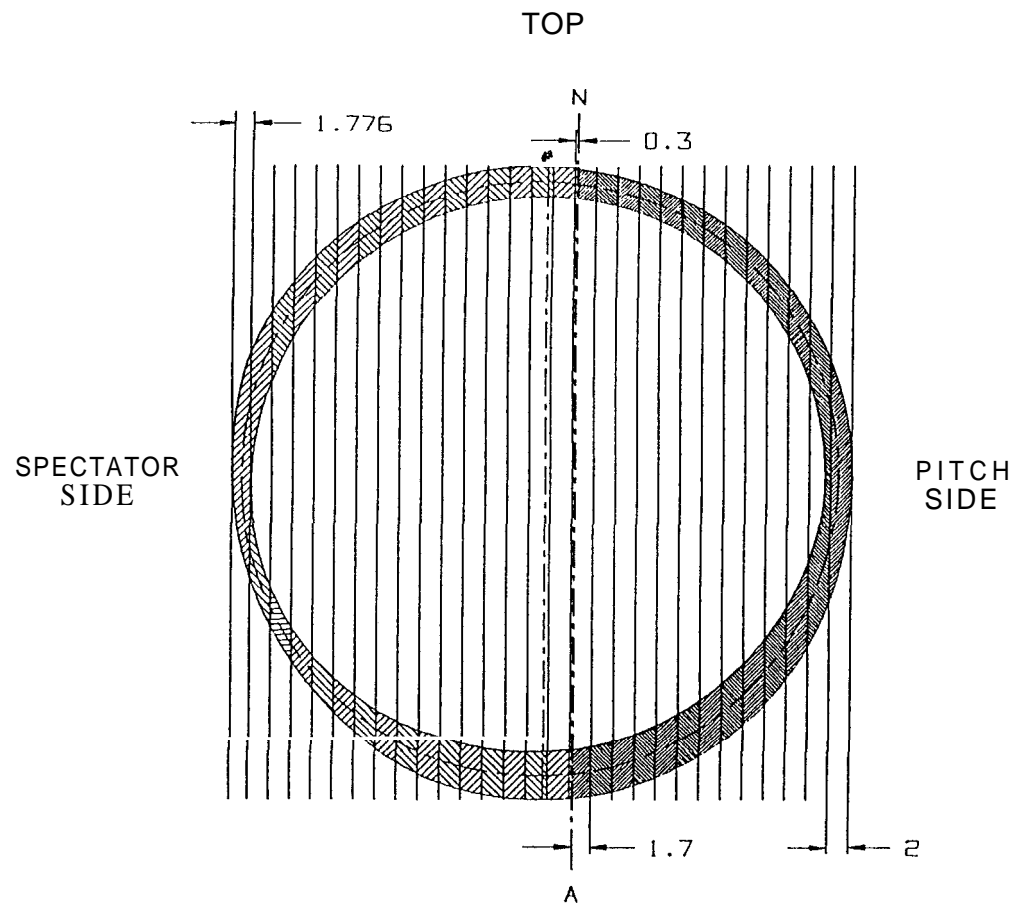
TOTAL PLASTIC SECTION MODULUS = 8504.349 mm^3

No	AREA (Al)	L (mm)	AREA (Ab)	(Al+Ab) xL	TOTAL
1	4.913	0.85	7.818	10.821	–
2	5.818	2.70	9.339	40.924	51.745
3	5.902	4.70	9.535	72.554	124.299
4	6.068	6.70	9.691	105.583	229.884
5	6.251	8.70	9.982	141.227	371.111
6	6.513	10.70	10.329	180.209	551.321
7	6.742	12.70	10.689	221.374	772.695
8	7.265	14.70	11.232	271.906	1044.601
9	7.967	16.70	11.639	327.420	1372.021
10	8.921	18.70	12.919	408.408	1780.429
11	10.955	20.70	14.329	523.379	2303.808
12	17.678	22.70	20.262	861.238	3165.046
13	29.574	24.70	–	730.478	3895.523
				TOTAL	3895.523

No	AREA (Al)	L (mm)	AREA (Ab)	(Al+Ab) xL	TOTAL
1	0.895	0.15	1.370	0.340	–
2	5.764	1.30	9.044	19.250	19.950
3	5.848	3.30	8.950	48.833	68.424
4	5.914	5.30	8.765	77.799	146.222
5	5.991	7.30	8.733	107.485	253.707
6	6.187	9.30	8.669	138.161	391.868
7	6.309	11.30	8.534	167.726	559.594
8	6.570	13.30	8.298	197.744	757.339
9	6.871	15.30	7.840	225.079	982.416
10	7.133	17.30	7.315	249.950	1232.367
11	7.602	19.30	6.943	280.718	1513.086
12	8.045	21.30	6.576	311.427	1824.513
13	9.033	23.30	6.255	356.210	2180.723
14	9.917	25.30	6.231	408.544	2589.268
15	11.966	27.30	6.665	508.626	3097.894
16	16.029	29.30	9.610	751.223	3849.117
17	24.359	31.188	–	759.708	4608.825
				TOTAL	4608.825

Fig A2.3   BARRIER No 124A SPAN 3/4 END No 3

DW SWFC6M

TOP

N

1.56 1.62

PITCH
SIDE

SPECTATOR
SIDE

0.38 2

A
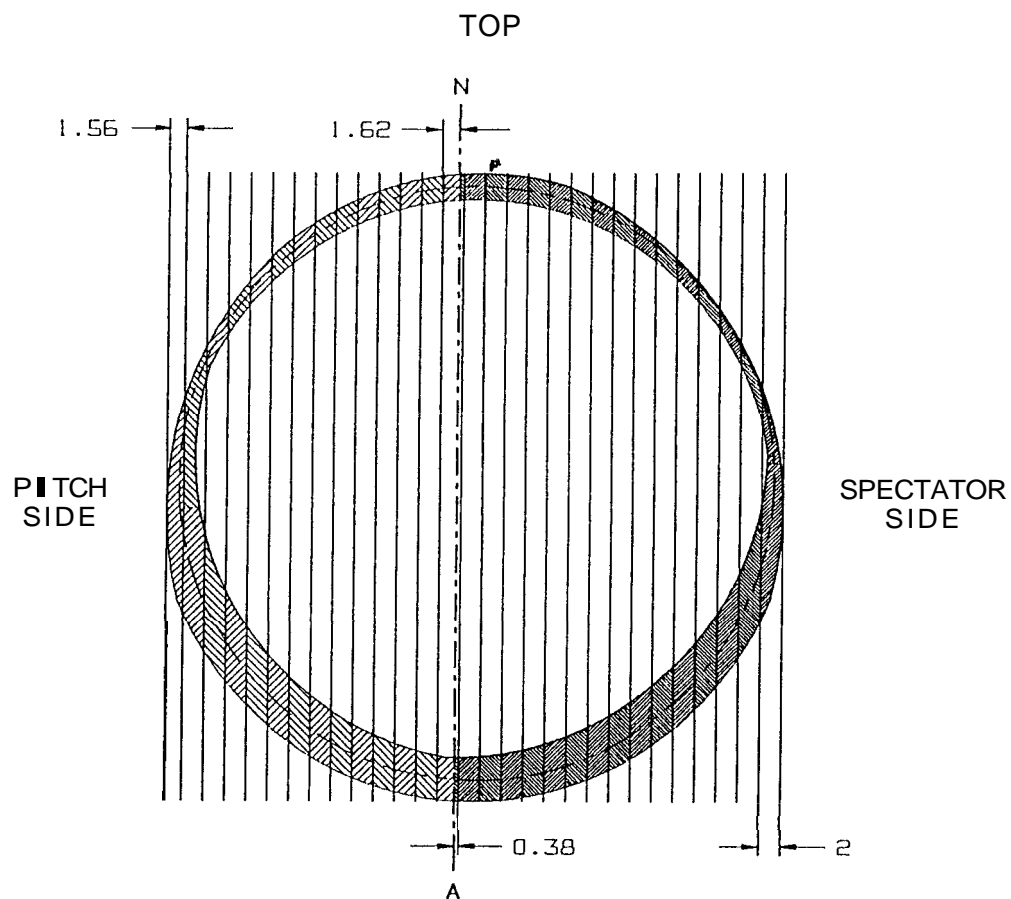
TOTAL PLASTIC SECTION MODULUS = 8268.929 mm^3

No	AREA (Al)	L (mm)	AREA (Ab)	(Al+Ab) xL	TOTAL
1	0.937	0.19	1.551	0.473	–
2	4.982	1.38	8.321	18.358	64.704
3	5.050	3.38	8.522	45.873	64.704
4	5.172	5.38	8.776	75.040	139.744
5	5.274	7.38	9.037	105.615	245.360
6	5.386	9.38	9.319	137.933	383.292
7	5.173	11.38	9.626	168.413	551.705
8	4.876	13.38	10.022	199.335	751.040
9	4.539	15.38	10.248	227.424	978.464
10	4.286	17.38	10.855	263.151	1241.615
11	4.101	19.38	11.464	301.650	1543.265
12	3.924	21.38	12.181	344.325	1887.590
13	3.924	23.38	13.304	402.791	2290.380
14	4.204	25.38	14.939	485.849	2776.230
15	5.363	27.38	18.001	639.706	3415.936
16	27.350	29.38	–	803.543	4219.479
				TOTAL	4219.479

No	AREA (Al)	L (mm)	AREA (Ab)	(Al+Ab) xL	TOTAL
1	3.960	0.81	6.532	8.498	–
2	4.863	2.62	8.368	34.665	43.164
3	4.764	4.62	8.788	62.610	105.774
4	4.744	6.62	9.131	91.852	197.626
5	4.748	8.62	9.723	124.740	322.366
6	4.70	10.62	10.241	158.673	481.040
7	4.686	12.62	10.792	195.332	676.372
8	4.699	14.62	11.612	238.467	914.839
9	4.716	16.62	12.552	286.994	1201.833
10	4.582	18.62	13.940	344.880	1546.713
11	4.532	20.62	15.832	419.906	1966.619
12	4.985	22.62	19.324	549.870	2516.489
13	17.487	24.62	22.814	992.211	3508.699
14	20.483	26.10	–	540.751	4049.450
				TOTAL	4049.450

Fig A2.4 BARRIER No 124A SPAN 3/4 END No 4

DH SWFC7M

APPENDIX 3

A 'LEANING CROWD' MODEL TO ESTIMATE THE LOADS GENERATED BY A BARRIER

Consider a person on the nth step behind a barrier. The whole crowd is assumed to be up on its toes, inclined forward at an angle 8, in a fashion which would be adopted to obtain a view of an incident in front of the crowd. The spectator is leaning forward on a support provided by the person in front and is thus subject to supporting force P_n from the front and to a toppling force P_{n-1}, from the person behind, offset by the terrace step height h.
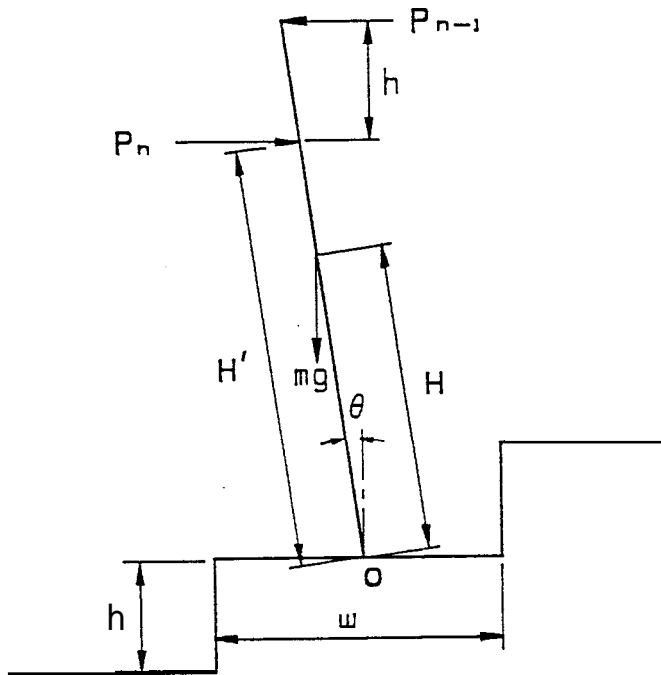
h = Step Height

H = Centre of Mass Height

H' = Push Height

w = Step Width

mg = Weight of Spectator

Equilibrium of person on the nth step, moments about O

$$P_n H' \cos\theta = mgH\sin\theta + P_{n-1}(H'\cos\theta + h)$$

$$P_n = mg(H/H')\tan\theta + P_{n-1}(1 + h/(H'\cos\theta))$$

ie a recurrence relationship of the form:

$$P_n = A + BP_{n-1}, \quad A, B \text{ constants}$$

$P_0 = 0$
$P_1 = A$
$P_2 = A + AB$
$P_3 = A + AB + AB^2$
- -
$P_n = A + AB + AB^2 + \ldots\ldots + AB^{n-1}$

$P_n = A(B^n - 1)/(B-1)$ (Sum of geometric progression)

$$P_n = \frac{mg\,H\,\sin\theta}{h}\left[\left[1 + \frac{h}{H'\cos\theta}\right]^n - 1\right]$$

For the person immediately behind the barrier, if the barrier is at the push height, then clearly P, would be transmitted to the barrier. In general the barrier is lower than this, and the push is probably transmitted to the barrier by bending at mid-height for the few rows of people just behind the barrier. If this were not so, the person at the barrier would be subjected to a large turning moment. The exact details of this force feed to barrier height are not yet clear, but for this purpose it is assumed that P,, where n is the number of steps behind the barrier in question, is the force on the barrier.

If the crowd density is N/sq m, then there are Nw persons/unit length on each step, thus we obtain the force/unit length on the barrier as:

$$\text{Force/unit length} \quad = \frac{N\ w\ mg\ H\ \sin\theta}{h}\left[\left[1 + \frac{h}{H'\cos\theta}\right]^{n} - 1\right]$$

which is the expression evaluated on Fig 2. A 'lean' angle of 10 deg has been estimated as a reasonable value to use in the calculation; other parameters are declared on the Figure.

It should be noted that no previous work can be found in the literature concerning this type of calculation. Existing design rules for barriers appear to rely on empiricism together with limited experimental testing. Caution should be exercised in the use of this new model, which requires experimental substantiation.